# Measuring the Spin-Polarization Power of a Single Chiral Molecule

*Albert C. Aragonès, Ernesto Medina,* Miriam Ferrer-Huerta, Nuria Gimeno, Meritxell Teixidó, Julio L. Palma, Nongjian Tao, Jesus M. Ugalde, Ernest Giralt,* Ismael Díez-Pérez,* and Vladimiro Mujica**

Electron transport in chiral systems exhibits a number of remarkable features having to do with the fact that spin–orbit interaction induces a coupling between the linear momentum and the spin of electrons, which translates into the appearance of spin polarization and spin filtering. The phenomenon is called electron dichroism as, in many ways, it is the equivalent of the better-known optical dichroism effect. In the latter, it is the rotation of the plane of polarization of the magnetic and electric components of the electromagnetic field that is experimentally measured, whereas the former corresponds to the polarization of the electronic spin. The phenomenon is also known as chirality-induced spin selectivity (CISS),[1] inferring that the transport of one of the electronic spins is facilitated over the other in a chiral structure.

In its simplest description, CISS in a molecular junction can be considered as a one-electron scattering process due to the molecular electrostatic potential of the chiral structure. In photoemission experiments, electrons are photoexcited from a metal surface and transmitted through a self-assembled monolayer of chiral molecules;[2] whereas in the case of local scanning probe microscopies (SPM), there is a transport process of electrons under a bias voltage through the junction.[3] Both experimental situations, photoemission and SPM, can be thought of as tunneling processes with energies above or below the work function of the material, respectively. In photoemission experiments, the spin polarization of the ejected electrons has been directly measured, and it has been found that very large polarization factors can be obtained starting with an unpolarized electron state.[2] In the case of SPM measurements, the manifestation of spin polarization is a change in the observed conductance, e.g. measurable spin-dependent threshold voltage of the charge transport through the junction.[3]

In this article, we report on a striking experimental manifestation of CISS in a single-molecule scanning tunneling microscopy (STM) break-junction, consisting of individual peptide molecules of well-defined chirality bridged between a magnetized STM Ni tip and an Au electrode. These experiments constitute the first reported case of observed current asymmetries in single chiral molecular junctions using the STM break-junction technique, where the statistics of many single-molecule measurements are collected and represented in a conductance histogram. It is important to mention, in this context, the pioneering work by Naaman and co-workers, which showed, using a completely different

A. C. Aragonès, M. Ferrer-Huerta, N. Gimeno, Prof. I. Díez-Pérez
Department of Material Science and Physical Chemistry
University of Barcelona
Barcelona, 08028 Catalonia, Spain
E-mail: isma_diez@ub.edu

A. C. Aragonès, Prof. I. Díez-Pérez
Institute for Bioengineering of Catalonia (IBEC)
Barcelona, 08028 Catalonia, Spain

A. C. Aragonès, Prof. I. Díez-Pérez
Centro Investigación Biomédica en Red (CIBER-BBN)
Campus Río Ebro-Edificio I+D
Poeta Mariano Esquillor s/n, 50018 Zaragoza, Spain

Prof. E. Medina
Centro de Física
Instituto Venezolano de Investigaciones Cientificas (IVIC)
Apartado 21827, Caracas 1020A, Venezuela
E-mail: ernesto@ivic.gob.ve

Prof. E. Medina
School of Physics Yachay Tech
Yachay City of Knowledge
100119 Urcuqui, Ecuador

DOI: 10.1002/smll.201602519

Dr. M. Teixidó, Prof. E. Giralt
Institute for Research in Biomedicine (IRB Barcelona)
Barcelona Institute of Science and Technology (BIST)
Baldiri Reixac 10, 08028 Barcelona, Spain
E-mail: ernest.giralt@irbbarcelona.org

Dr. J. L. Palma, Prof. N. Tao, Prof. V. Mujica
Arizona State University School of Molecular Sciences
Physical Sciences Center PSD-D102 and Biodesign
Institute Center for Bioelectronics and Biosensors
Tempe, AZ 85287, USA
E-mail: vmujica@asu.edu

Prof. J. M. Ugalde, Prof. V. Mujica
Donostia International Physics Center (DIPC)
Manuel Lardizabal Ibilbidea, 4, 20018 Donostia, Gipuzkoa, Spain

Prof. E. Giralt
Departament de Química Orgánica
Universitat de Barcelona
Barcelona, 08028 Catalonia, Spain

junction architecture, that nanoscale molecular junctions formed by trapping few DNA molecules between an Au nanoparticle and an Ni ferromagnetic surface display current asymmetries as a function of the direction of the Ni magnetic polarization.[3]

The control of two experimental variables, the magnetization orientation of the Ni tip and the chirality of the peptide, allows probing the three key physical asymmetries of the junction regulating its conductance: magnetoresistance, chirality, and spinterface (interfacial magnetism arising as a result of the metal/molecule interaction), and they allow us to extract a value of the spin-polarization power (capability to spin-polarize electrical current) of a single chiral molecule of ≈60%. These experiments can be understood and rationalized in terms of a theoretical model that connects spin polarization with transport in molecular junctions recently developed by Medina and co-workers, which generalizes the well-established Landauer model for electron transport in metal–molecule–metal junctions to include the filtering effect of the molecular chirality and the presence of a magnetized electrode.[4,5]

The combined theoretical and experimental analysis affords a novel way to estimate the molecular spin-polarization power, which is essentially the spin-dependent transmission probability, a magnitude that is directly linked to the single-molecule conductance.

We have measured the spin-dependent single-molecule conductance of an $\alpha$-helical peptide sequence of 22 amino acid (AA) residues of both L- and D-isomers (see **Figure 1**), employing a spin-polarized version[8] of the STM break-junction approach.[6–8] The procedure is based on driving a magnetically polarized STM Ni tip in and out of contact to/from an Au(111) substrate functionalized with the target peptide immersed in a helical-inducing liquid medium (TFE(2,2,2-Trifluoroethanol)/$H_2O$: 60/40 v/v[9]). During the contact process, individual peptides can spontaneously bridge between both biased electrodes via two –S terminal groups (see Figure 1).[10] The current was recorded for each pulling stage in the form of current versus time/displacement, and all traces

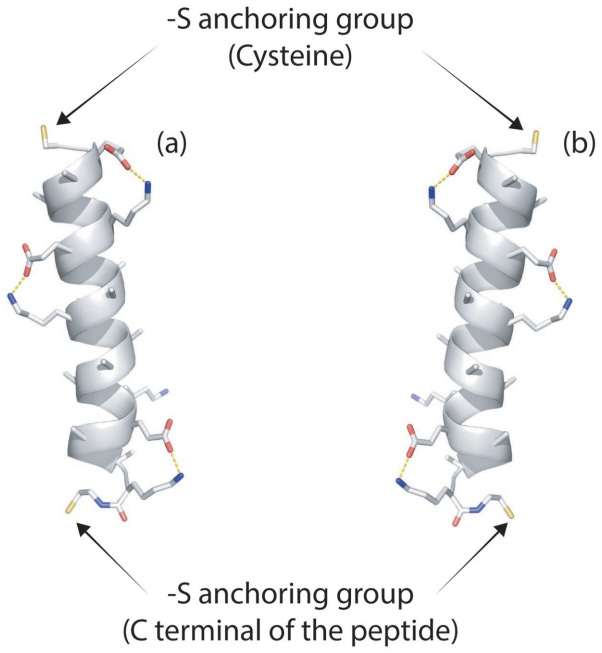


Amino acid sequence:
H-CEAAAKEAAAKEAAAKEAAAK-NH-$CH_2$-$CH_2$-SH

**Figure 1.** Secondary structure of the dextrorotatory (D-) (a), and levorotatory (L-) (b) $\alpha$-22AA-peptides and the amino acid sequence synthesized in this work.

displaying well-defined single-molecule plateau features (see **Figure 2**) were used to build a conductance histogram.[6] The observed maxima represent the most probable conductance values for the formed single-molecule contact (see Section S6 in the Supporting Information for more details).

In the single-peptide transport measurements, we focus on the three key physical parameters of our model (Figure 2): (1) the chirality of the molecular backbone, which

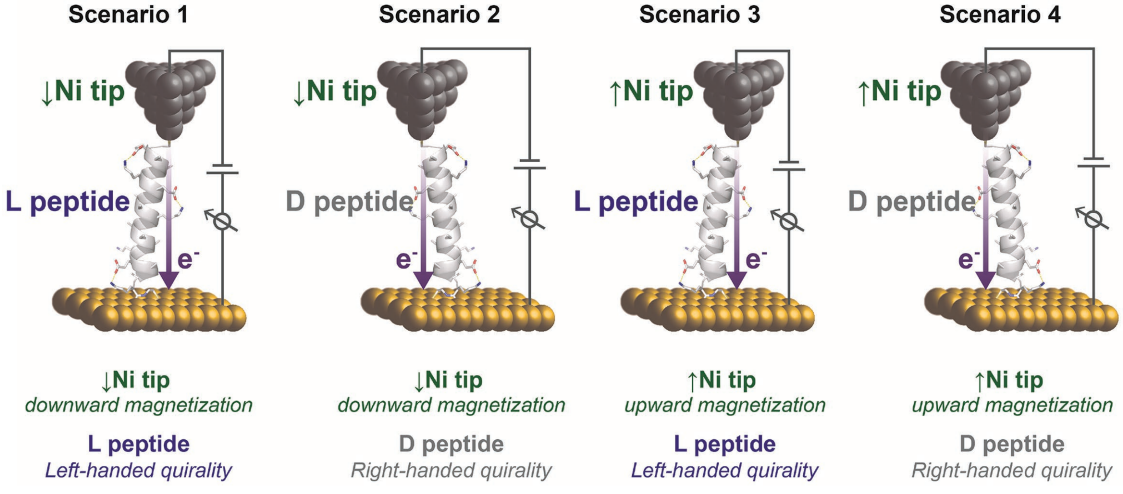


**Figure 2.** Schematic representation and description of the four studied case scenarios combining the three key experimental parameters. Sample bias voltage (defined as sample minus tip voltages) is positive meaning the electrons are flowing from the Ni to the Au electrodes.

is introduced by measuring the D- and L-enantiomers (for synthetic details see Supporting Information, Section S5); (2) the initial polarization state, which is defined by using premagnetized Ni STM tips in both directions along the main junctions' axis; and (3) inherent magnetization at the molecule/electrode interface due to the strongly polarizing nature of the Au–S bond (spinterface).[8,11–13]

We present here the results of the four case scenarios where the electrons are injected from the Ni-polarized source into the chiral peptide backbone and drained through the bottom Au electrode (see Figure 2). These cases are the most representative ones of the observed spin-dependent transport through the chiral molecular structures. The four cases corresponding to the opposite bias voltage (current being injected from the nonmagnetic Au bottom electrode) also show spin-dependent transport effects and they are analyzed in the Supporting Information (section S2) within the same model framework. The single-peptide conductance histograms in **Figure 3**a,b show that when the magnetic polarization of the Ni tip is reversed, the conductance for the D- and L-isomers switch the order, being the highest and the lowest conductance sets for the L- and D-isomers, respectively, both under "spin-up Ni magnetization direction". These experimental observations will be contrasted to the different scenarios described within the framework of our model below.

We have developed a theoretical model for the description of CISS, which clearly establishes that this phenomenon is the result of the combined effect of broken space inversion symmetry due to chirality, spin–orbit interaction, and broken time reversal symmetry by an external bias that selects a preferential direction for electron injection (see related experimental results in the Supporting Information, Section S2). These conditions are satisfied in all instances of experimental setups where CISS has been observed, i.e., electron photoemission, electron transport in molecular junctions, and intramolecular electron transfer.[2,3,14]

In presenting the simplest version of a theoretical model that accounts for a quantitative interpretation of the experimental results we need to explicitly connect spin polarization with conductance. To this end, we consider that electron transport occurs via a one-electron tunneling mechanism under the Landauer regime, where the current is well described by a dimensionless transmission coefficient $\tau(E,V)$, which depends on the nature of the tunneling barrier (see experimental assessment on the transport mechanisms in Supporting Information, Section S1)

$$I(V) = \frac{4e}{h}\int_{\mu_L}^{\mu_R} \mathrm{d}E\,\tau(E,V) \tag{1}$$

where $E$ is the energy of the tunneling electron, $V$ is the applied bias voltage, and $\mu_L$ and $\mu_R$ are the electrochemical potentials in the left and right electrodes, respectively. In the linear regime of low bias voltage, which is the one we will be concerned with here, Equation (1) becomes

$$I(V) = \frac{4e^2}{h}\tau(E_F)V \tag{2}$$

In this regime, the conductance is given by the Landauer expression

$$G = \frac{4e^2}{h}\tau(E_F) \tag{3}$$

where the transmission coefficient can be written as

$$\tau(E_F) = T_{LMR}\,g_L(E_F)\,g_R(E_F) \tag{4}$$

and $T_{LMR}$ is the effective coupling to the left (L) and (R) electrodes mediated by the molecule M and $g_{L/R}(E_F)$ are the densities of states of the L/R electrodes at the Fermi energy. The effective coupling is a product of the term connected to the propagation of electrons through the molecule, and the coupling of the molecule to the electrodes.

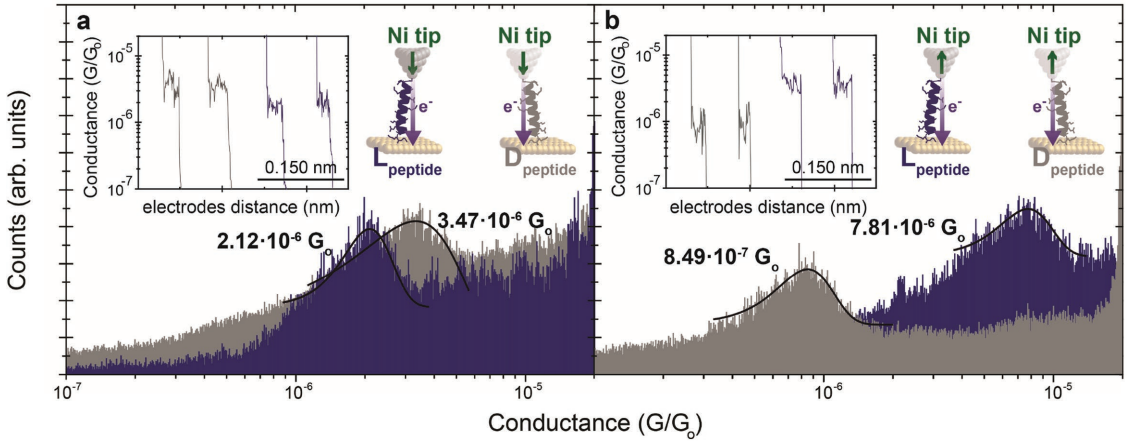


**Figure 3.** Semilog conductance histograms (counts vs $G/G_0$, $G_0$ being the conductance quantum equal to 77.5 μS) for the dextrorotatory and levorotatory $\alpha$-22AA-peptides under spin down a) and up b) Ni magnetic polarizations. The short green arrows indicate the Ni-tip magnetization direction while the violet arrows indicate the electron injection direction. The conductance values were extracted from Gaussian fits from the histogram peaks. The applied sample bias was set to +50 mV. Insets show representative current versus pulling traces used to build the conductance histograms.

  

In the presence of spin-polarization effects, Equation (4) has to be modified in several ways. First, the transmission coefficient needs to include information about the spin state of the electrons entering the junction. Second, an explicit dependence on the chirality of the molecule must be included. Third, an explicit indication of the helicity of the electronic state must be given. The helicity of an electronic state is specified by the projection of the spin vector in the direction of propagation, i.e., by the scalar product $s \cdot k/(|k||s|) = \pm 1$. Fourth, the contact density of states (DOS) also depends on spin in a way that will be specified below. We include this information by adding three subindices to the notation for the transmission coefficient, i.e., $\tau_{M,\mathbf{k},\mu}$, where the molecular index $M$ can take the values D and L; k indicates the propagation direction; and $\mu = \pm 1$ is the helicity index.

We have shown that the transmission coefficient obeys the important symmetry constraints, assuming that the D isomer filters out the negative helicity state

$$\begin{aligned} &\tau_{\mathrm{D},\mathbf{k},+} = \tau_{\mathrm{D},-\mathbf{k},+};\ \tau_{\mathrm{L},\mathbf{k},-} = \tau_{\mathrm{L},-\mathbf{k},-} \\ &\tau_{\mathrm{D},\mathbf{k},-} = \tau_{\mathrm{L},\mathbf{k},+} = 0 \end{aligned} \tag{5}$$

where the first relations correspond to the Kramers doublets and the preservation of time-reversal symmetry in the absence of an external bias, and the second relations represent the filtering conditions, i.e., a high handicap to transport for the filtered out spin component. The essential physical content of these relations is that chiral molecules are filters of electronic state helicity rather than electronic spin.

In the presence of an external bias, which forces a specific injection direction, either +k or –k, time-reversal symmetry is broken and the chiral molecule acts as a spin filter in the direction of propagation, i.e., each optical isomer selects an electron spin polarization (fixed by helicity).

The conductance through the peptide from the Ni to the Au contact is controlled by two factors according to Equation (4): the product of the densities of states of each contact $g_{m_s}^{\mathrm{Au,Ni}}(\varepsilon_F)$ evaluated at the Fermi level for either the Au or the Ni, where $m_s$ denotes the spin orientation quantum number, and the effective coupling $T_\sigma^{\mathrm{helix}}(k)$, which is the spin-dependent tunneling matrix element of the peptide. In addition to the tunneling process through the molecule and the density of states at the contacts, there is an interfacial magnetic effect that in practice imposes an energy penalty to polarized electrons. A specific model of this phenomenon, referred to as spinterface, has been extensively used.[8,15] Such a coupling produces a spin-dependent bias voltage that changes the effective conductance of the molecular junction. This effect is small compared to the molecular filtering properties and the DOS spin-imbalance at the Fermi energy of the magnetic contact; however, it must be included to fully describe the experimental observations.

We now write the full spin-dependent conductance as

$$G_{m_s} = \frac{4e^2}{h}\tau_{m_s} \tag{6}$$

where the spin-dependent transmission coefficient is given by

$$\tau_{m_s} = T_{m_s}^{\mathrm{helix}} g_{m_s}^{\mathrm{Au}}(\varepsilon_F) g_{m_s}^{\mathrm{Ni}}(\varepsilon_F)\left[1 + m_s \frac{\mu_{sN}}{V}\right] \tag{7}$$

where $\mu_{sN}$ is the excess chemical potential produced by spin–charge coupling between the Au substrate and the anchoring group, $V$ is the applied voltage to the Au contact, and the $m_s$ factor implies that one spin orientation adds a voltage while the other subtracts it. $\mu_{sN}$ is a spin-dependent voltage that accelerates electrons of one spin, and it does not depend on the chirality of the molecule but only on the nature of the magnetic interface.[8,16] The associated voltage to the spin–charge coupling favors injecting spin up into the molecule, while by the same token favors withdrawing spin down from the molecule.

Equation (6) is a fundamental result connecting, in an explicit way, spin polarization and conductance. In fact, it allows estimating the spin-polarization power of a molecule, the analog of the optical rotational power in photon dichroism, by simply dividing the conductances corresponding to the two optical isomers in a chiral junction. This aspect of the theoretical model will be further explored in a forthcoming publication.

Regarding the $T_\sigma^{\mathrm{helix}}(k)$ according to the theory,[17] the spin–orbit interaction coupled to the chirality of the helix generates a gap between two Kramers doublet states (four states combining two propagation directions and two spin orientations) with well-defined helicity.[4,5] We consider that, in our experiments, the electronic state helicity (spin) is strongly selected through this mechanism.

Regarding the DOS of the metallic contacts, in the case of Au, there is no discrimination according to the electron spin, so Au emits or accepts electrons of both orientations equally well except for the extra spin–charge voltage described by $\mu_{SJ}$ due to the anchoring group. On the other hand, Ni displays a large contrast between the minority and the majority spin DOS.[18] According to the DOS of nickel, there is a handicap for injecting or emitting the majority spin as compared to the minority spin. With these ingredients we can understand the results shown in Figure 3.

**Figure 4** summarizes, within the frame of previous arguments, the conductance hierarchy according to favorable/unfavorable transmitted electron spin toward the chiral peptide or the spin–charge voltage. The corresponding experimental values of the conductances (Figure 3) have been organized in ascending values in the bottom $X$-axis. The Ni electrode is assumed to inject minority spin electrons in the junction according to its spin-polarized DOS distribution near the Fermi level. The helicity state chosen by the chiral molecule is that L-isomers (D-isomers) carry positive (negative) helicity. One can readily see that the two higher conductances correspond to the preferred spin by the peptide, being the larger conductance value the one that sees the preferred spin for the spin–charge effect as well. The two smaller conductances correspond to the unfavorable directions for the chiral peptide, again in order of preference of the spin–charge effect. With these results, we can disentangle the larger chiral effect in the spin-dependent transport of these single-peptide junctions versus the spinterface effect due to the spin–charge voltage. For the case of the current in the Au to Ni direction, the conductance hierarchy can be understood in the same terms (see Supporting Information, Section S2).

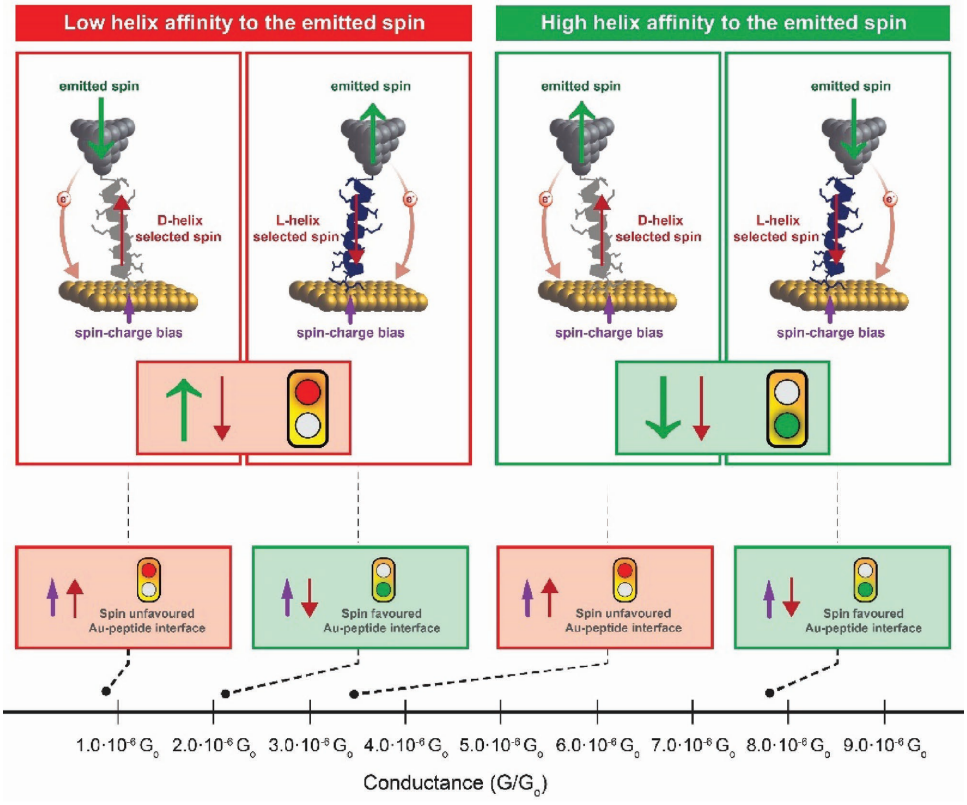


**Figure 4.** Transport of electrons from the Ni to the Au electrodes. We order the experimental values of the conductance in the X axis, increasing to the right. The binary lights signal the resistance to electron transfer; green is the lower and red is the higher resistor as described in the text. The D peptide supports negative helicity (spin antiparallel to current sense) while the L peptide supports positive helicity transport (spin parallel to current sense). The central light refers to the electron helicity selected by the chiral molecule, while the small bottom light refers to the spin–charge voltage effect, which always favors down spin versus up spin when injected to the Au.

A straightforward application of the above-mentioned conceptual framework allow us to calculate the polarization power for each isomer (L or R) as the asymmetry factor between the currents flowing through the same isomer for the two opposite Ni electrode magnetic polarizations

$$SP_{L/R}(\%) = \frac{G^{>}_{L/R} - G^{<}_{L/R}}{G^{>}_{L/R} + G^{<}_{L/R}} \quad (8)$$

where $G^{>}$ and $G^{<}$ are the high and low conductance levels for each isomer. A simple calculation yields $SP_L = 60\%$ and $SP_D = 57\%$, which are remarkably similar within the experimental accuracy. Theoretically, one should also expect similar results since the symmetry breaking and spin–orbit effects responsible for the phenomenon are molecular in origin. It is interesting to notice that these values are comparable to those measured in electron photoemission experiments with DNA for much larger chains.[2] This raises the unresolved question as to whether the spin-polarization effect for transport at energies above and below the work function is the result of purely coherent process (tunneling) or includes an incoherent mechanism (hopping).

The helicity preference is contemplated by the theory elsewhere.[4,5,17] A source of asymmetry not explicitly discussed, nevertheless, is the direction of the always-present dipole moment along the oligopeptide axis. Eckshtain-Levi et al.[19] have shown that one indeed reverses the selected spin by reversing the molecule (e.g., oligopeptides based on alanine[20]). This result comes most likely from the difference in electron affinity between the molecule and the gold surface generating a net charge transfer and a large fixed electric dipole for all the configurations studied. In terms of the model, the dipole could make the Rashba term larger than the intrinsic spin–orbit interaction and yield a dipole orientation-dependent filter. This is an issue for further study.

In summary, we have established, for the first time, a direct verification of the spin filtering capabilities of chiral molecules using a break-junction STM technique, in an asymmetric magnetic single-molecule junction, consisting of a magnetized Ni tip, a Au electrode, and a chiral molecule. The results are strikingly consistent with a modified Landauer transport theory that takes into account the properties of the magnetic contact, the helicity selection of the chiral filter, and the interfacial effects induced by chemical bonding. The theoretical model is capable of explaining the experimental results for the eight different scenarios determined by the variation in the three control variables: the direction of the voltage in the junction, the spin selection of the chiral molecule, and the polarization of the Ni tip.

The strong rectification effects observed in the limit of zero voltage conductance confirm the molecular nature of the spin filtering effect, even in the absence of the electric field associated with the bias, and the huge potential of

  

chiral filters as circuit components in spintronics devices. They also offer an experimental glance at a deep connection between spin polarization and tunneling transmission, which affords a direct assessment of the molecular spin-polarization power, a topic that we will address in depth in a forthcoming publication.

The implications of our findings for the general field of electron transport through chiral media are considerable, especially in the field of electron transfer in biological systems, because the same physical mechanism responsible for the spin-induced rectification effects in the junction underlie the fact that spin polarization provides for a mechanism to lower the transmission tunneling barriers in molecules.

## Supporting Information

*Supporting Information is available from the Wiley Online Library or from the author.*

## Acknowledgements

*This research was supported by the MINECO Spanish National Projects (Grant Nos. CTQ2015-71406-ERC, CTQ2015-64579-C3-3-P, BIO2013-40716-R, and CTQ2013-49462-EXP) and Generalitat de Catalunya (XRB, 2014-SGR-1251, and 2014-SGR-521). V.M. acknowledges the generous support of the Donostia International Physics Center during his Sabbatical Year. V.M. is grateful to Prof. Mark Ratner for inspiring discussions about the subject. E.M. acknowledges Dr. Werner Bramer for useful observations. I.D.-P. thanks the Ramon y Cajal program (MINECO, No. RYC-2011-07951) for financial support. A.C.A. thanks the Spanish Ministerio de Educación for an FPU fellowship. IRB Barcelona and IBEC are recipients of a Severo Ochoa Award of Excellence from MINECO (Government of Spain).*

[1] S. G. Ray, S. S. Daube, G. Leitus, Z. Vager, R. Naaman, *Phys. Rev. Lett.* **2006**, *96*, 36101.
[2] B. Göhler, V. Hamelbeck, T. Z. Markus, M. Kettner, G. F. Hanne, Z. Vager, R. Naaman, H. Zacharias, *Science* **2011**, *331*, 894.
[3] Z. Xie, T. Z. Markus, S. R. Cohen, Z. Vager, R. Gutierrez, R. Naaman, *Nano Lett.* **2011**, *11*, 4652.
[4] S. Yeganeh, M. A. Ratner, E. Medina, V. Mujica, *J. Chem. Phys.* **2009**, *131*, 14707.
[5] E. Medina, F. López, M. A. Ratner, V. Mujica, *EPL* **2012**, *99*, 17006.
[6] B. Xu, N. J. Tao, *Science* **2003**, *301*, 1221.
[7] N. J. Tao, *Nat. Nanotechnol.* **2006**, *1*, 173.
[8] A. C. Aragonès, D. Aravena, J. I. Cerdá, Z. Acís-Castillo, H. Li, J. A. Real, F. Sanz, J. Hihath, E. Ruiz, I. Díez-Pérez, *Nano Lett.* **2016**, *16*, 218.
[9] B. P. Orner, X. Salvatella, J. Sánchez Quesada, J. De Mendoza, E. Giralt, A. D. Hamilton, *Angew. Chem. Int. Ed. Engl.* **2002**, *41*, 117.
[10] S. Sek, K. Swiatek, A. Misicka, *J. Phys. Chem. B* **2005**, *109*, 23121.
[11] S. Trudel, *Gold Bull.* **2011**, *44*, 3.
[12] A. Hernando, P. Crespo, M. A. García, E. F. F. Pinel, J. de la Venta, A. Fernández, S. Penadés, M. A. Garcia, A. Fernandez, S. Penades, *Phys. Rev. B* **2006**, *74*, 52403.
[13] R. Gréget, G. L. Nealon, B. Vileno, P. Turek, C. Mény, F. Ott, A. Derory, E. Voirin, E. Rivière, A. Rogalev, F. Wilhelm, L. Joly, W. Knafo, G. Ballon, E. Terazzi, J.-P. Kappler, B. Donnio, J.-L. Gallani, *ChemPhysChem* **2012**, *13*, 3092.
[14] P. C. Mondal, C. Fontanesi, D. H. Waldeck, R. Naaman, *ACS Nano* **2015**, *9*, 3377.
[15] F. Al Ma'Mari, T. Moorsom, G. Teobaldi, W. Deacon, T. Prokscha, H. Luetkens, S. Lee, G. E. Sterbinsky, D. A. Arena, D. A. MacLaren, M. Flokstra, M. Ali, M. C. Wheeler, G. Burnell, B. J. Hickey, O. Cespedes, *Nature* **2015**, *524*, 69.
[16] J. Fabian, A. Matos-Abiague, C. Ertler, P. Stano, I. Žutić, *Acta Phys. Slovaca. Rev. Tutorials* **2007**, *57*, 342.
[17] S. Varela, V. Mujica, E. Medina, *Phys. Rev. B* **2016**, *93*, 155436.
[18] E. Tsymbal, *Handbook of Spin Transport and Magnetism*, Chapman & Hall/CRC: Boca Raton, FL, USA **2011**.
[19] M. Eckshtain-Levi, E. Capua, S. Refaely-Abramson, S. Sarkar, Y. Gavrilov, S. P. Mathew, Y. Paltiel, Y. Levy, L. Kronik, R. Naaman, *Nat. Commun.* **2016**, *7*, 10744.
[20] I. Carmeli, V. Skakalova, R. Naaman, Z. Vager, *Angew. Chem. Int. Ed. Engl.* **2002**, *41*, 761.

Received: July 28, 2016
Revised: September 8, 2016
Published online: October 18, 2016

  